

1 **An Open-Source Toolbox for investigating functional resilience in sewer networks based on**
2 **global resilience analysis**

3 Behnaz Kamali^a, Ali Naghi Ziaei^{a,1}, Aliasghar Beheshti^a, Raziye Farmani^b

4 ^a Department of Water Science and Engineering, College of Agriculture, Ferdowsi University of Mashhad (FUM),
5 Mashhad, Iran.

6 ^b Department of Engineering, University of Exeter, Exeter EX4 4QF, UK.

7 **Abstract**

8 Resilience analysis of urban infrastructures such as sewerage systems is very important due to
9 different stressors. Failure in these infrastructures may lead to economic, social, health and
10 environmental consequences. The functional resilience of systems can be analyzed in all failure
11 levels caused by unpredictable or even unknown events based on the global resilience analysis
12 (GRA) method. To perform GRA under different scenarios of pipe collapse and blockage, the
13 performance of the system must be evaluated in all possible link failure combinations. The time
14 of this process might be unfeasibly long in real sewerage networks. In this paper, an open-source
15 toolbox is developed which uses a proposed scenario selection method based on roulette wheel to
16 perform GRA without simulating all possible scenarios. This toolbox is based on a proposed O-
17 SWMM API which is a developed version of EPA's Storm Water Management Model (SWMM)
18 to optimize simulation time and memory usage. The results show that the mean resilience for a
19 sample and also a real sewer network was estimated by the proposed method with RMSE less than
20 0.025 and 0.022 respectively comparing with simulating all possible scenarios. Moreover, the
21 GRA computation using O-SWMM API was at least 2.26 times faster than SWMM.exe.

¹ Corresponding author.
E-mail address: an-ziaei@um.ac.ir

22 **Keywords:** Global resilience analysis, Storm Water Management Model, Scenario reduction, Roulette
23 wheel, Multi criteria decision making, Open-source toolbox.

24 **1. Introduction**

25 Many infrastructure systems such as sewer networks must be investigated in exceptional
26 conditions. Because, failure of these systems can lead to serious economic, social, environmental,
27 and health consequence (Davis et al. 2013). The origin of the word resilience is the Latin word
28 "resiliere", which means to "bounce back" (Hosseini et al. 2016). Doorn et al. (2019) used a formal
29 concept for the resilience. They defined performance of resilience as the ability to keep or enhance
30 certain functions. This concept was used by Chen et al. (2021) to develop a methodology for
31 quantifying the resilience of hazardous storage systems. Mottahedi et al, (2021) suggested the
32 definition of “the ability of a critical infrastructure system exposed to hazards to resist, absorb,
33 accommodate to and recover from the effects of a hazard in a timely and efficient manner, for the
34 preservation and restoration of essential services” for evaluating resilience. Cai et al. (2021)
35 defined the resilience as the ability of systems to recover quickly after external disruptive events.

36 In this paper the definition of resilience in Butler et al. (2014) is used. They defined resilience
37 as “the degree to which the system minimizes level of service failure magnitude and duration over
38 its design life when subject to exceptional conditions”.

39 Risk analysis is commonly summarized as incorporating both the probability of an event and the
40 consequences (Johnson et al. 2021). However, various events threaten sewer networks which some of them
41 are unknown or unpredictable and the probability of their occurrences cannot be determined (Sweetapple
42 et al. 2018). Moreover, each event might have several different consequences or different events can lead
43 to the same end states (Johansson et al. 2011). Therefore, this paper focused on a middle state analysis.

44 The middle state analysis method evaluates the system performance based on consequences
45 caused by different and unknown threats and emphasizes on response of the level of service
46 provision to system failure. It is more easily identifiable and measurable than identification and
47 analysis of multiple threats. In the middle state analysis, the consequences of the events that result
48 in the same system failure mode can be addressed with a single analysis regardless of their type to
49 represent all the potential modes of failure. Therefore, it enables a more comprehensive resilience
50 assessment and improves the adaptation development process (Butler et al. 2016).

51 Johansson et al. (2011) presented a method for the global vulnerability analysis (GVA) of
52 technical infrastructures and used it for an empirical analysis of the electrical distribution systems.
53 Mugume et al. (2015) introduced global resilience analysis (GRA) in urban drainage network
54 based on the middle state approach. The GRA investigates the network at all different failure levels
55 (number of failed links) from zero to 100 percent in order to analyze resilience of network in different
56 level of consequences. This method has four steps. Firstly, the failure mode (i.e., sewer collapse or
57 blockage) needs to be identified. In the second step, the system stress (percentage of failed
58 components i.e., earthquake, oil clogging) associated with the failure mode and the simulation
59 manner are identified. Then, the system corresponding strain (resulting loss of system functionality)
60 is detected and determined how to measure it. And finally, the failure mode strains are simulated
61 under increasing stress magnitude up to 100 percent of maximum stress (Mugume et al. 2015).

62 Sweetapple et al. (2018) presented a GRA toolbox for water distribution systems based on
63 EPANET software application, but there is no toolbox for analyzing global resilience in sewer
64 networks. In sewer networks, conduit blockages due to accumulation of sediment, fat, oil, and
65 grease, or tree root penetration, can cause the sewage to be overflow in residential areas (Davis et
66 al. 2013). Although, these threats are related to operations and management, the critical blockages

67 due to some threats such as earthquakes and floods can cause blockage in a large number of links
68 in the sewer networks (Hughes et al. 2020). This number can be much more than 5 to 10 percent,
69 especially in earthquake-prone countries such as Iran (Kamranzad et al. 2020). Heavy storms in
70 combined networks can also cause similar consequences. These events are not generally
71 predictable and thus, the consequences of all possible scenarios must be investigated. Such analysis
72 is computationally expensive and quickly becomes complex for even small systems (Johnson et
73 al. 2021). Therefore, in sewer networks with large number of conduits and manholes, simulation
74 of all possible scenarios (GRA) is unaffordable in some circumstances.

75 Mugume et al. (2015) used the sequential random link selections method for sewer networks in
76 order to overcome GRA's computational challenges. Diao et al. (2016) proposed a semi random
77 selection method for GRA and applied it to water distribution systems. In their method, at each
78 stress magnitude a fixed number of failure scenarios are generated randomly and $2[c - (c_f - 1)]$
79 number of failure scenarios are generated in a targeted manner, where c and c_f are total and failed
80 components, respectively. Atashi et al (2020) also used the same selection method as Diao et al.
81 (2016) to determine the total number of scenarios in order to evaluate the resilience of water
82 distribution systems based on location of isolation valves. In Diao et al. (2016), the total number
83 of scenarios is directly related to the number of links in the network but Mugume et al. (2015) used
84 a convergence analysis method to determine the required number of scenarios. Therefore, this
85 number is different for each sewer network and is based on the characteristics of that network.

86 Although, this approach is used to specify sufficient number of random selections, but
87 improving the selection method can generate results that are closer to the resilience computed
88 using all possible scenarios. Finding the scenarios generating lowest and highest resilience in each
89 failure level can lead to achieving this goal.

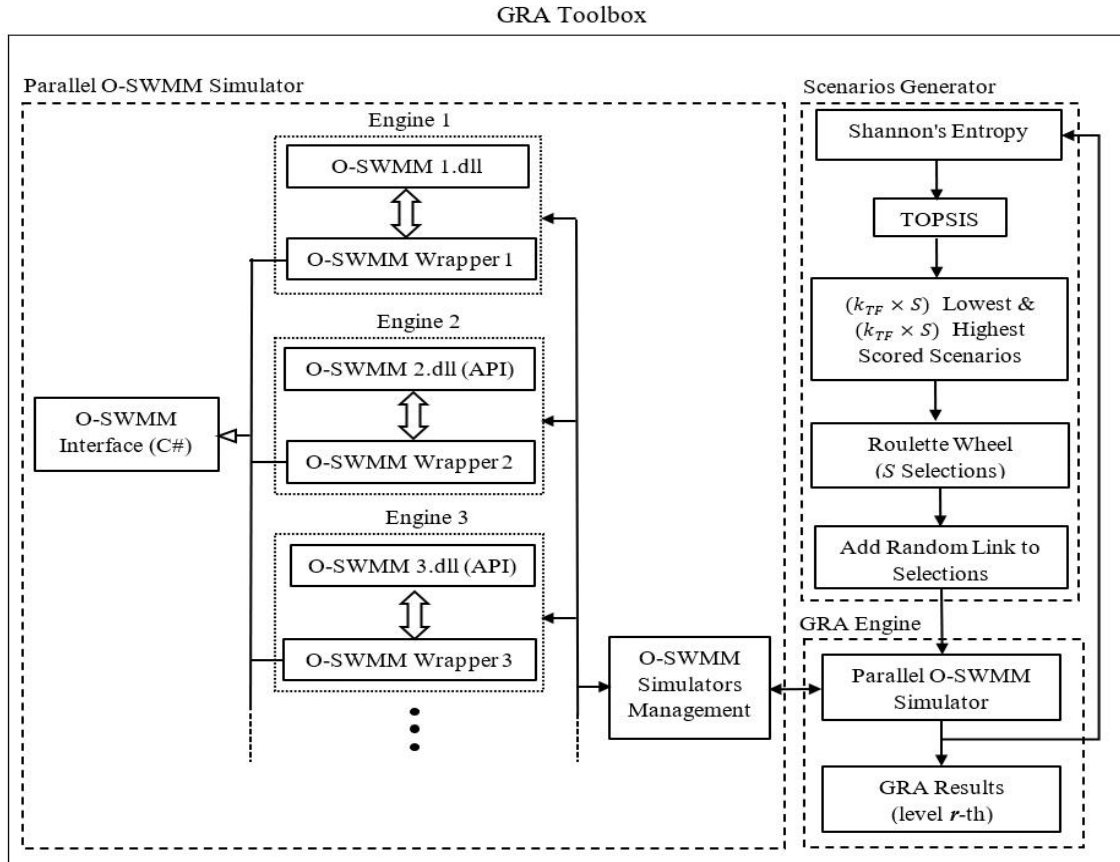
90 In this study, a toolbox is presented for GRA in sewer networks which make a trade-off between
91 time and reliability of results using a proposed multi criteria selection method based on roulette
92 wheel. This method finds the scenarios with lowest and highest resilience in each failure level
93 named as strategical scenarios and uses them to generate the scenarios of the next failure levels.
94 The toolbox is able to simulate the selected scenarios based on a development of the SWMM
95 engine to reduce simulation time of each scenario.

96 **2. Parallel GRA toolbox**

97 In this study, an open-source toolbox is proposed in C# language for analyzing global resilience
98 of complex sewer networks². This toolbox simulates the sewer systems using a developed engine
99 which is based on SWMM (Storm Water Management Model).

100 The toolbox consists of three main blocks (Fig.1): scenario generator, parallel O-SWMM
101 simulator and GRA engine. The scenarios generator block generates the compendious set of
102 scenarios using a proposed multi criteria selection method based on roulette wheel. The generated
103 scenarios at each failure level are simulated via parallel O-SWMM block, which contains several
104 simulation engines (called simulator). Finally, the global resilience of sewer networks is
105 determined by GRA engine block. These blocks are more described in the following sub-sections.

² Availability: <https://github.com/BehnazKamali/OSWMM-GRA-Toolbox>



106

107

Figure 1: Block diagram of O-SWMM Toolbox

108 2.1 Parallel O-SWMM

109 2.1.1 Optimized-SWMM

110 SWMM is a dynamic rainfall-runoff model which has been developed by USEPA to simulate
 111 the performance of urban drainage and sewer networks. Although, its graphical interface simplifies
 112 usage of this engine, but it cannot be used in GRA because it requires multiple runs of model
 113 simulation. This justifies the utilization of SWMM engine (e.g., SWMM5.exe or SWMM API³) in
 114 an auxiliary software. Macro et al (2019) used this method to develop a tool for connecting

³ An Application Programming Interface (API) is a collection of entry functions included in the software interface that allows external applications to call them directly for interacting with software components.

115 SWMM.exe⁴ engine and an optimization software in order to implement green infrastructure.
116 Banik et al (2014) developed a SWMM toolkit based on SWMM API for sewer systems to identify
117 pollution source using genetic algorithm. In SWMM API, a number of exportable functions⁵ have
118 been provided to communicate with SWMM engine before, during and after a model simulation.
119 Riano-Briceno et al (2016) presented an open-source toolbox named as MatSWMM in which some
120 getters, setters⁶ and data management functions were developed, because they needed to modify
121 the setting of several orifices during the simulation and create for example a graph data
122 structure from the network. Therefore, to change parameter values such as link properties during
123 simulation and also tailor the outputs to suit specific needs, new exportable functions should be
124 defined in SWMM engine. Moreover, in this engine there is no way to manage output file's content
125 such as simulation's report file. If there are some getter functions by which the values of the desired
126 variables can be obtained, then there is no need to report file or at least it can be summarized.
127 Writing in a file is also a time-consuming part in each program; especially, when it needs to be
128 repeated several times or is required to be shared among parallel processors.

129 However, Open Water Analytics group [<http://wateranalytics.org>] provided a series of
130 exportable functions to customize the use of SWMM engine, but new exportable functions are
131 proposed in our developed engine called Optimized-SWMM (O-SWMM) to get and set the value
132 of some attributes before and also during the simulations (Table 1). Moreover, two report file
133 management functions were considered to reduce hard drive overhead.

⁴ SWMM.exe is executable SWMM engine which can be executed directly or run by an auxiliary application in windows.

⁵ Exportable function is a type of functions which are defined in the software API for using by external applications.

⁶ Getters and setters are API's functions (accessor properties) which are used for accessing value of properties and modifying their values.

134 The `swmm_setLinkGeom` function which sets the geometry parameters of a link was first
 135 proposed by Martínez-Solano et al. (2016) based on EPA SWMM 5.0.022 source code, but their
 136 library is not open source and does not work with input files⁷ created by new versions of SWMM.
 137 The proposed O-SWMM was developed based on EPA SWMM 5.1.013 source code. Its
 138 possibility of changing Manning's n or pipe diameter before and also during simulation can be
 139 used in evaluating completely failure scenarios (such as GRA) or partial failure scenarios which
 140 are considered in the design of sewer networks to achieve better performance. In the GRA result
 141 section, this possibility is used and also significant reduction in simulation time and reducing
 142 volume of data needing to be written to the hard disk is reported using O-SWMM API.

Functions	Description
<code>swmm_getLinkGeom</code>	Gets values of xsection parameters
<code>swmm_setLinkGeom</code>	Sets values of xsection parameters
<code>swmm_getConduitLinkRoughness</code>	Gets Roughness (Manning's n) of a conduit
<code>swmm_setConduitLinkRoughness</code>	Sets Roughness (Manning's n) of a conduit
<code>swmm_setAverageDWFChangingCoef</code>	Sets a specific coefficient to change DWF inflow
<code>swmm_getLinkXsectType</code>	Gets link's xsection type
<code>swmm_getObjectCount</code>	Gets count of specific type of SWMM objects (nodes, links...)
<code>swmm_getRouteModel</code>	Gets flow routing method
<code>swmm_getNodeInflow</code>	Gets total inflow volume to a node
<code>swmm_getOccuredNodeFlooding</code>	Determines whether there has been a flood in the nodes so far
<code>swmm_setGenerateReportFile</code>	Determines whether the report file is generated or not
<code>swmm_setReportFlags</code>	Sets report flags to determine which parts should be included in the report file

143 Table 1: Functions included in O-SWMM Toolbox

⁷ The input (.inp) file is the file format for SWMM. It contains the wastewater network properties and simulation parameters.

144 2.1.2 Parallel Implementation

145 Some efforts have been made to parallelize the SWMM engine to increase the simulation speed
146 of sewer systems (Burgess et al. 2000, Burger et al. (2014)). Burger et al. (2014) have considered
147 four options of parallelization: multiple models, multiple events, multiple time step computation
148 and multiple algorithms. They focused on the third option in which computation of conduits within
149 a time step is distributed among available cores. The results show that the simulation time is
150 decreased by 6 to 10 times on a twelve-core system. However, they estimated that the maximum
151 speedup that can be achieved on any system is about 15 times regardless of the number of available
152 threads. But, Mair et al., (2014) showed that by using first option for simulating several
153 independent models, the result of parallelism is globally close to optimal time. In this parallelism
154 level, the number of concurrent simulations and degree of speed increases are directly related to
155 number of available cores and total time of simulating is absolutely reduced by adding number of
156 cores. Therefore, in Parallel O-SWMM block, this parallelism structure was adopted to simulate
157 independent scenarios in each GRA failure level.

158 In Parallel O-SWMM block, the number of concurrent executable simulations depends on
159 available logical processors. Logical processors are the number of cores times the number of
160 threads that can run on each core through the use of hyperthreading. Management of these logical
161 processors is performed by the O-SWMM engine's management block. Whenever a logical
162 processor is released, the O-SWMM engine's management block assigns another simulation
163 scenario to that logical processor. For implementing this ability in Visual Studio, all of the O-
164 SWMM wrappers in the block inherit from an object named O-SWMM interface and each of them
165 is communicated to its own O-SWMM.dll API (Fig. 1).

166 2.2 Scenario Generation

167 One of the advantages of GRA method is evaluating system performance in a wide range of
168 hydraulic failure scenarios. Considering each link has two possible cases: non-failed and complete
169 failure cases, the total number of conduit failure scenarios in the entire solution space is calculated
170 as:

$$171 \quad F(N, c_i) = \sum_r \frac{N!}{(N-r)!r!} \quad r = 1, \dots, N \quad (1)$$

172 where r and N are the failure level and the total number of sewer network's links, respectively.

173 In real sewer networks, considering all possible combinations of conduit failure makes the
174 computation very time consuming or even impossible. One of the possible solutions is to generate
175 scenarios randomly. In this method, interdependent network components (links) are blocked
176 randomly with equal failure probability for all components (Almoghathawi et al. 2019). Mugume
177 et al. (2015) showed that for an 81-link urban drainage system (UDS), by considering more than
178 200 random failure scenarios the deviation percentage of GRA results are not significant, in all
179 failure levels. It means that, for each failure level if a sufficient number of scenarios are selected
180 randomly, the average resilience for them is approximately equal to the average resilience of all
181 possible scenarios for that failure level.

182 All possible scenarios of each failure level can be divided into two sets. The first set includes
183 the extreme scenarios also called strategical scenarios of that failure level in this paper, are
184 scenarios where the resilience function takes on an extreme value. But, the second set includes
185 scenarios whose resilience values are close to each other. This set can be generated using the
186 random method proposed by Mugume et al. (2015). Therefore, in order to obtain more accurate
187 GRA results with affordable time and computational cost it is necessary to use an efficient scenario
188 selection method which is able to discover the extreme scenarios (first set) in each failure level.

189 In this study, a simple multi criteria scenario selection method based on a roulette wheel is
190 introduced to find scenarios which lead to the minimum and maximum resilience at each failure
191 level. The Roulette/Spinning wheel (RW) method as a selection operator is often used in genetic
192 and evolutionary algorithms. In this method, a slice of the wheel is assigned to each individual,
193 according to its fitness. In the presented GRA toolbox, each scenario in any failure level plays the
194 role of the individuals. The extreme scenarios from individuals of one failure level are named as
195 strategical scenarios, because these scenarios participate in generating individuals of the next
196 failure level. The goal is that the scenarios generated for the next failure level include the extreme
197 scenarios of the current level.

198 In each failure level, the probability of a scenario being strategic is estimated by a RW's fitness
199 function. In sewer networks, the fitness function can be resilience but it should not be used for
200 evaluating scenarios when multi-criteria participate in scoring scenarios. For example, suppose
201 that a number of scenarios in a failure level have the same resilience based on function of the flood
202 volume and failure time terms. So, if this function is used as fitness function, then these scenarios
203 have the same slice size in RW. But they may have different flooding loss and failure time values,
204 individually. Under this same condition, the weights of terms are usually determined in order to
205 use in a Multi-Criteria Decision Making (MCDM) method using experimental studies based on
206 questionnaire results or entropy, the Analytic Hierarchy Process (AHP), Analytic Network Process
207 (ANP), or Best Worst Method (BWM) methods (Maghsoodi et al. 2018). In this paper, the entropy
208 method which was proposed in 1948 by Shannon (Shannon, 1948) is used, because it can quantify
209 the amount of information in each criterion based on the criterion values distribution. The criterion
210 with more entropy is more important. So, the weight of this criterion in fitness function method is
211 more than weights of other criteria (Long et al. 2019). Then scenarios are scored based on a fitness

212 function such as the Technique of Order Preference Similarity to the Ideal Solution (TOPSIS)
213 (Hwang et al, 1993). In this method, first a positive ideal and a negative ideal solution were found
214 and then the distance of each option from these solutions are calculated based on criteria values.
215 The criteria can be positive or negative in nature. Wang et al. (2017) proposed a new framework
216 based on TOPSIS to support decision making in sustainable drainage systems scheme design. For
217 this, they used 12 criteria such as resilience, hydraulic performance and costs.

218 In the proposed GRA scenario selection method, the aim is to look for scenarios that are close
219 to negative or positive ideal solutions. So, scenarios with lowest and highest scores are preferred.
220 But this method requires a pre-processing step to determine the weights of the criteria.

221 According to these concepts, the GRA scenario selection algorithm includes the following steps
222 at failure level r (Fig. 1):

- 223 1. Assuming that S scenarios were simulated at failure level $r - 1$, the weights of criteria using
224 Shannon entropy are determined.
- 225 2. The S scenarios are scored using TOPSIS method with respect to criteria weights obtained
226 from previous step. The fitness scores are normalized between 0 to 1.
- 227 3. $k_{TF} \times S$ number of these scenarios with the lowest scores and $k_{TF} \times S$ with the highest
228 scores are selected, where k_{TF} is an arbitrary coefficient between 0 and 1. These two sets of
229 scenarios are participated in scenario generation process of next failure level r .

230 Notice: In the first failure level, all the possible scenarios are considered and simulated.

- 231 4. The roulette wheel is generated based on fitness scores of the selected scenarios. For the
232 scenarios with highest scores, the size of slices is equal to the scores, but for the scenarios
233 with the lowest scores, the size of slices is equal to the $1 - score$. This is because the

234 probability of choosing them must be equal to the probability of choosing the scenarios with
235 the highest scores in the proposed selection method.

236 5. A random scenario is selected from the generated roulette wheel. This candidate is a
237 combination of $r - 1$ conduits.

238 6. A random conduit (except of the conduits in the candidate scenario) is added to the scenario
239 in order to generate scenario of the next failure level.

240 7. Steps 5 and 6 are repeated to generate a set of S distinct scenarios of the failure level r .

241 It should be mentioned that for simple sewer network, value of S at each failure level r can be
242 the number of distinct r -combinations of conduits, obtained from Eq.1. But for complex networks,
243 value of S can be a fixed value for all failure. Although, the number of distinct r -combinations of
244 conduits at failure levels 1, $N - 1$ and N are equal to N , N and 1, respectively. In these failure
245 levels, all of the combinations are simulated by the GRA toolbox.

246 **2.3 GRA Engine**

247 After generating S scenarios for a failure level, these scenarios are simulated by parallel O-
248 SWMM simulator. Then, resilience is calculated for each of these scenarios by a predefined
249 resilience formula proposed by Mugume et al., (2015):

$$250 \text{ Res}_i = 1 - \sum_{j=1}^n \left[\frac{V_{Fj}}{V_T} \times \frac{t_{Fj}}{t_T} \right] , i = 1, \dots, S \quad (2)$$

251 where i and j are number of scenarios in each failure level and number of flooded nodes in each
252 scenario, respectively. V_T and V_{Fj} are the total inflow volume and the flood volume occurred in
253 node j , respectively. t_{Fj} is failure duration of node j and t_T is simulation time. It should be noted
254 that this equation is used to verify the toolbox performance, and can be substituted by another

255 formula upon need. For example, Nan and Sansavini (2017) proposed a metric which integrates
256 six measures defined based on system resilience transitions in order to evaluate the resilience in
257 interdependent infrastructures. Sharma et al. (2018) proposed simple metrics (e.g., Center of
258 Resilience and Resilience Bandwidth) that decompose the recovery curve for resilience
259 quantification. Moreover, Wang et al. (2019) presented a new approach for assessing resilience of
260 urban drainage systems using resilience profile graph which unify the concepts and metrics of
261 reliability, robustness, resilience and failure. Cheng et al. (2021) reviewed the resilience metrics,
262 along with their limitations and applicable scenarios. They developed multimodal resilience
263 metrics including instantaneous resilience at specific time instants, overall resilience and average
264 resilience over a time period. The system reliability, average robustness and average recovery
265 ability were considered in their proposed metrics.

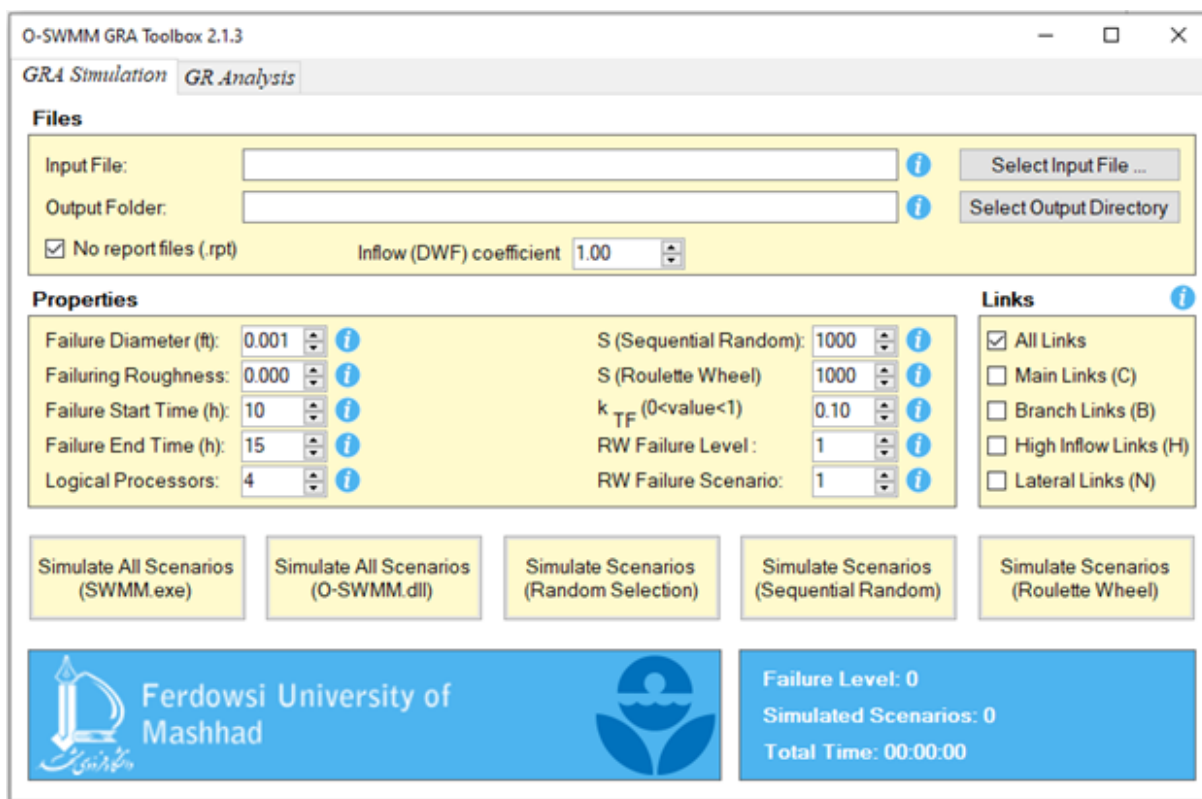
266 Finally, the minimum, mean and maximum of these resilience values are calculated for each
267 failure level. When this process was executed for all failure levels, the global resilience is
268 illustrated vs failure levels.

269 **3. Results and discussion**

270 Figure 2 shows proposed toolbox user interface which has two tabs for simulating and analyzing
271 GRA results. Two types of blockage simulations can be considered on conduits by setting a non-
272 zero value for changing diameter or roughness parameters located in properties section. Start and
273 end time of failure are specified by failure start time and failure end time parameters based on
274 exportable function of O-SWMM API. Moreover, by changing the inflow (DWF) coefficient
275 parameter, the inflow values to the manholes can be increased or decreased in order to investigate
276 its effect on the resilience. The number of scenarios simulated in parallel is adjusted by logical
277 processors parameter and the value of S and k_{TF} related to scenarios generator block can be

278 adjusted in the properties section. In the links section, based on a predefined conduit naming rule
279 it can be specified which conduits can participate in the scenario generation process. This feature
280 is useful for extracting network skeleton from large urban sewage networks in order to decrease
281 number of possible scenarios.

282 Four different types of GRA simulation (GRA based on simulating all scenarios using
283 swmm.exe or O-SWMM API and also GRA based on simulating scenarios selected by two
284 different methods: proposed roulette wheel and random selection methods) were implemented on
285 the toolbox and used for analyzing two test cases to evaluate the performance of its blocks (Fig.
286 2). All processes executed using a laptop with the Intel(R) Core™ i7- 9750H CPU @ 2.60 GHz
287 and 8GB RAM. According to its CPU architecture, 10 out of the 12 available logical processors
288 were allocated to the Parallel O-SWMM block.



289

290

Figure 2: O-SWMM Toolbox User Interface

291 **3.1 Evaluation of O-SWMM API**

292 In the first experiment, an example network of EPA-SWMM’s manual (Gironás et al. 2010)
293 was used to evaluate functionality of O-SWMM API compared to the original SWMM application
294 (swmm.exe). Figure 3 shows a schematic view of the test case which includes a 29-hectare area
295 and variety of objects such as storage units, orifices, weirs and two typical Low Impact
296 Developments (LID).



297
298 Figure 3: Sample combined sewer system for toolbox validation

299 The network contains 20 nodes, 18 conduits and 24 sub catchments. Due to small number of
300 conduits, all possible combinations of failed links can be simulated in a fairly short time. Therefore,
301 262,143 simulations were performed using both EPA-SWMM and O-SWMM API for a 48-hour.
302 Moreover, the 100-year return period storm is selected from three existed events in order to
303 simulate an exceptional condition.

304 To run the EPA-SWMM similar to O-SWMM API, a C# auxiliary application was developed
305 such that multiple copies of swmm.exe could be run in a parallel manner. The structure of this

306 application is similar to “Parallel O-SWMM” block. For each failure scenario, a logical processor
307 generated an input file by modifying the roughness values of selected conduits to 100 in the
308 original input file and saved it on hard disk. Then, the related copy of swmm.exe was used to
309 simulate the generated input file (.inp) and the result was recorded in a report file ⁸(.rpt). When the
310 simulation of a scenario was completed, the report file was read by the logical processor to extract
311 the required information for GRA calculation. The same process was repeated for O-SWMM API,
312 except that by using proposed exportable functions, there was no need to further process for
313 generating input files and also writing and reading report files (.rpt). The roughness of selected
314 conduits was modified to 100 during runtime by using “swmm_setConduitLinkRoughness”
315 exportable function. It should be noted that, for accurate comparison the “reporting options”
316 property in original input file was set to “NONE” in order to decrease the process time of
317 swmm.exe simulation tools.

318 The execution time and size of written data for two simulation tools are shown in Table 2. As
319 it can be seen, the written data and consequently execution time are significantly decreased by
320 using O-SWMM API. When the SWMM.exe is used for global resilience analysis, the execution time
321 and size of written data is increased for each scenario simulation. Therefore, speed of processing is slowed
322 down because of file access. There are two clear reasons for this:

- 323 1. It is required that the input file is generated and written on the hard disk for each scenario simulation.
324 Because, each scenario has different conduits properties (diameter or Manning's n).

⁸ The report file is a plain text file in which SWMM simulation results include status and summary results reports are written.

325 2. The results of each simulation (.rpt file) are written on the hard disk by EPA SWMM and then the
326 GRA toolbox must be read the file in order to calculate resilience of each scenario based on the total
327 flooding loss and the flooding time.

328 These two time-consuming operations which have programming processing and also hard disk usage
329 are eliminated if the proposed exportable functions of O-SWMM API are used. Since conduits properties
330 are changed by `swmm_setLinkGeom` or `swmm_setConduitLinkRoughness` functions, a unique input file
331 for all scenarios is needed. After each simulation, the total flooding loss and the flooding time is gotten
332 using API functions, directly. So, we disabled writing report file on hard disk by
333 `swmm_setGenerateReportFile` proposed exportable function.

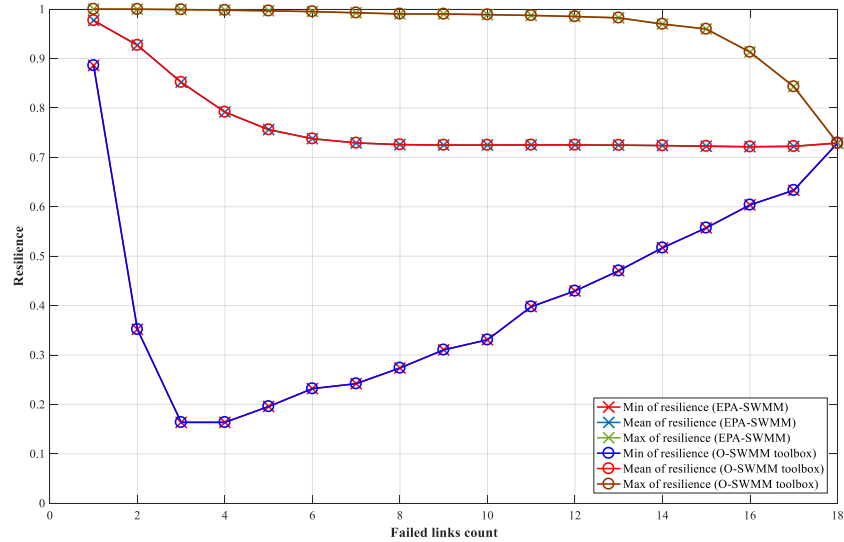
334

	Total Execution Time (min)	Data Written on Disk (MB)
335 SWMM.exe	806.15	18673
336 O-SWMM API	317.80	29

337 Table 2: Computational cost comparing between O-SWMM API and EPA-SWMM

338 In addition to computational cost, the GRA values calculated based on simulation results of O-
339 SWMM API and SWMM.exe were compared in order to evaluate performance accuracy of the
340 developed exportable functions of O-SWMM API. Figure 4 shows minimum, mean and maximum
341 of resilience values computed based on Eq. 2, at each failure level. The root mean square error
342 between obtained mean resilience values using two simulation tools was equal to $1.2275 e - 11$.

343 As the number of failed conduits increases, resilience is expected to decrease, but the results
344 show an increasing trend of the minimum resilience from failure level 4, in the sample network.
345 To investigate the rationale behind, two scenarios named as scenarios “A” and “B” were
346 considered.



347

348

Figure 4: Comparison of calculated resilience by EPA-SWMM and O-SWMM API

349

350

351

352

353

354

355

356

357

358

359

360

361

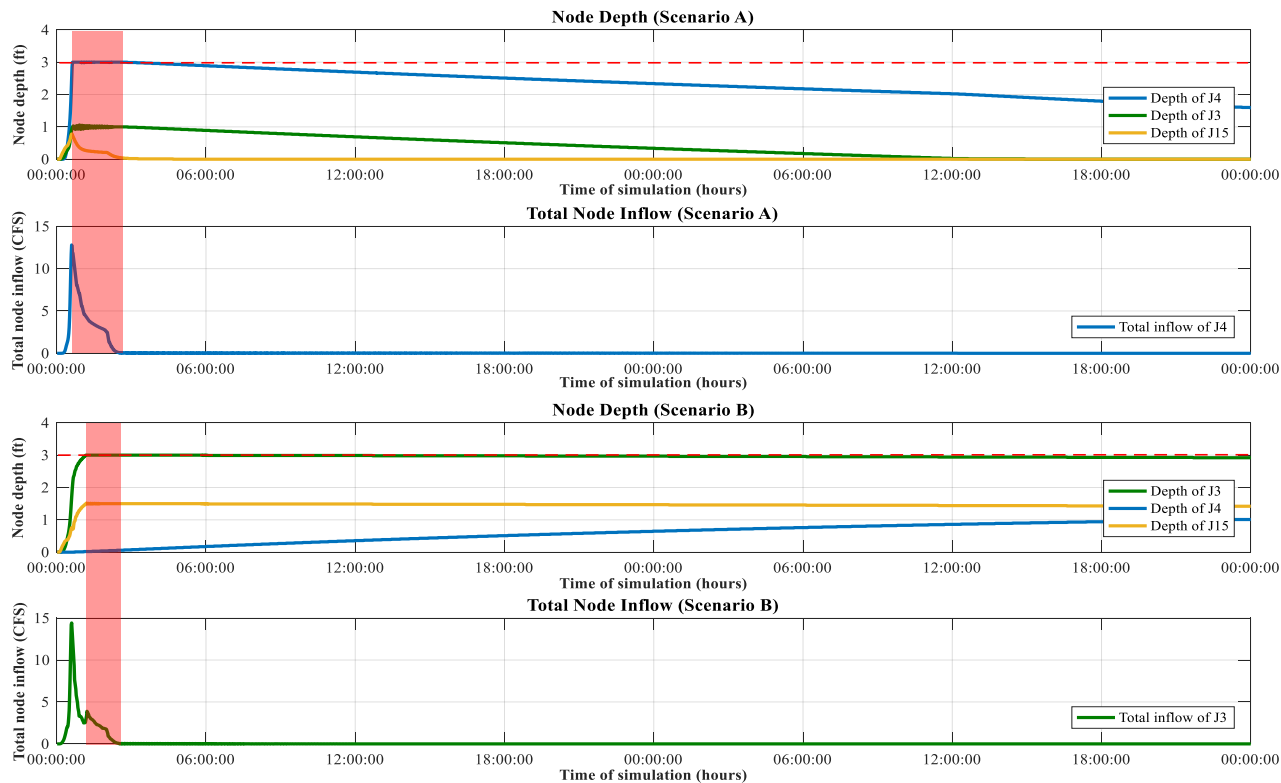
362

In the first scenario, conduit C4 was failed in two days. In the second scenario, conduit C4 and C3 were failed during same simulation time. In this sample network, junction depth of all three nodes J15, J3 and J4 is 3 ft. These conduits and nodes are shown in figure 3. The simulation results showed that in both scenarios one of these nodes was flooded, node J4 in scenario A and node J3 in scenario B. In the second scenario, the failure time was less than first one. The failure interval for each scenario is shown in figure 5 with a red highlight and it is about 1.42 and 1.16 hours for scenario A and B, respectively. Moreover, the total flood volume of scenario A is higher than scenario B. The flood volume for these scenarios was $12E4$ gallons and $4E4$ gallons, respectively. Therefore, according to equation 2 the resilience of scenario A with one failed conduit is less than scenario B in which two conduits were failed.

In this example, there were two reasons for increased resilience with increasing number of failed conduits. First, non-failed conduits can act as storage reservoir when other conduits are failed and retain some of the inflow. In the scenario B, conduit C15 stored about 33000 gallons during simulation time and a smaller amount of inflow entered to J4 because failed conduit C3

363 was not able to transfer sewage effluent. So, unlike to the scenario A flooding loss did not occur
 364 in J4. This was the second reason for the resilience increasing.

365 The node depth of the sewage effluent in three junctions J3, J4 and J15 during simulation time
 366 are shown in figure 5. The red dashed line shows allowed depth of effluent in these junctions. As
 367 it can be seen, the height of the sewage effluent in junction J3 is equal to the depth of this junction
 368 almost all along the simulation time. But, flooding loss at this junction is not occurred after 02:30
 369 on the first day, because the total inflow entered to this junction is zero from this time until the end
 370 of the simulation.

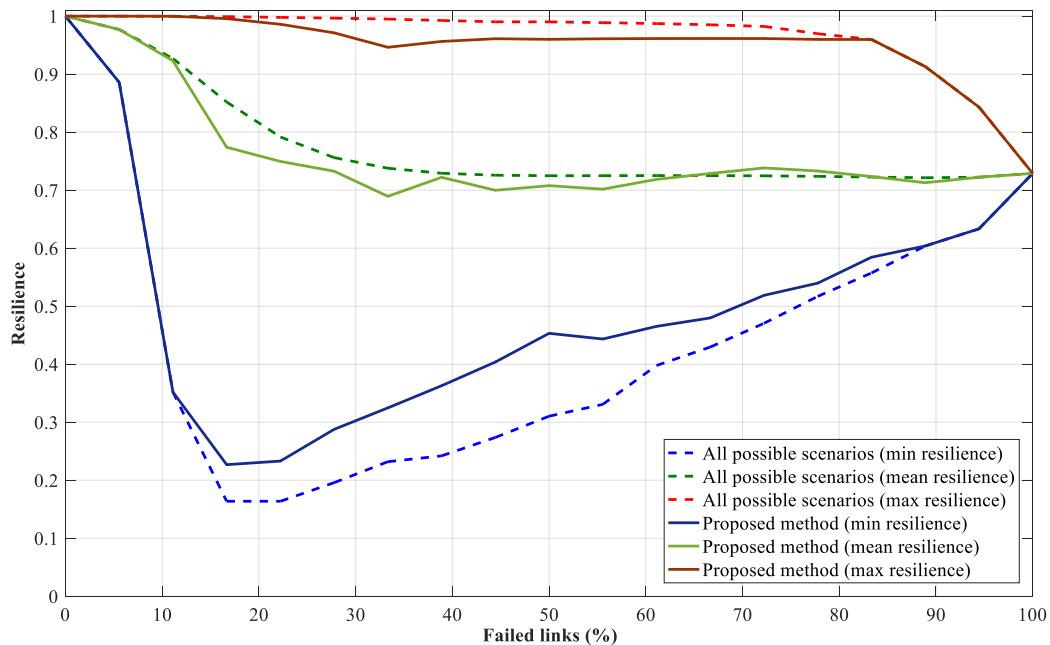


371
 372 Figure 5: Comparison of node depth and total inflow in two scenario A (blockage in C4) and B, (blockage in C3 and
 373 C4).

374 **3.2 Evaluation of Scenario Selection Approach**

375 To evaluate the proposed scenario selection method, the GRA results were compared with GRA
 376 results of simulating all possible scenarios in the mentioned sample network and also in a real
 377 sewer network.

378 In the first step, the toolbox was run to analyze global resilience of the sample network. The
 379 values of S and k_{TF} were considered to be 100 and 0.1 in the proposed scenario selection method.
 380 Moreover, two criteria (total flooding loss and mean failure time) were considered in Shannon
 381 entropy and TOPSIS processes to score simulated scenarios. The GRA results with this approach
 382 were then compared with all possible scenarios results (Figure 6). The minimum, mean and
 383 maximum resilience for the sample sewer network was estimated by proposed method with RMSE
 384 equal to 0.12, 0.08 and 0.02 which are quite satisfactory.



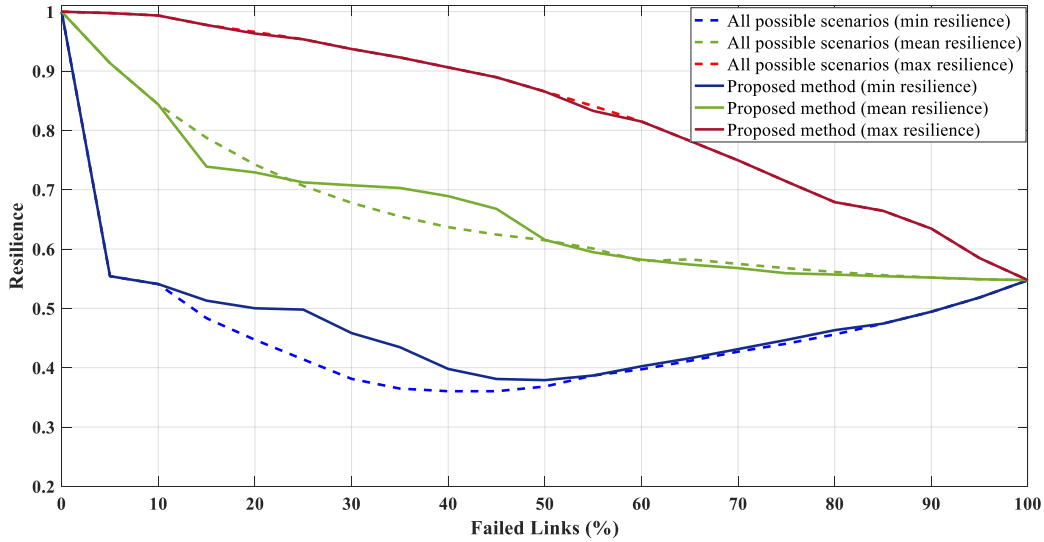
385
 386 Figure 6: Comparison of GRA results obtained from proposed selection method and all possible scenarios
 387 simulation for the sample sewer network.

388 Then performance of the presented GRA toolbox was evaluated in a real separate sewer system
389 for sanitary, a town in the north east of Iran. This fairly complex network (figure 7), consists of
390 1005 conduits and 999 nodes and designed for 42,000 citizens. Firstly, to make the simulation of
391 all possible scenarios achievable, 20 zones were identified in the network and their outlet conduits
392 were selected as representative conduits which participate in the failure scenarios. Figure 7 shows
393 these 20 zones in different colors and red circles represent conduits participated in GRA.



394
395 Figure 7: The real sewer network in Iran. The red circles indicate the representative links of each zone.

396 According to these 20 conduits, all 1,048,575 possible scenarios were simulated and GRA
397 results were calculated based on Eq. 2. The toolbox was then run in which the values of S and k_{TF}
398 were considered to be 100 and 0.1. The total flooding loss and mean failure time criteria were
399 considered in Shannon entropy and TOPSIS processes. Figure 8 has compared GRA results
400 calculated by selected scenarios using proposed method with all possible scenarios values. The
401 minimum, mean and maximum resilience for the real sewer network was estimated with RMSE of
402 0.033, 0.022 and 0.002 by simulating 20×100 scenarios, in overall.



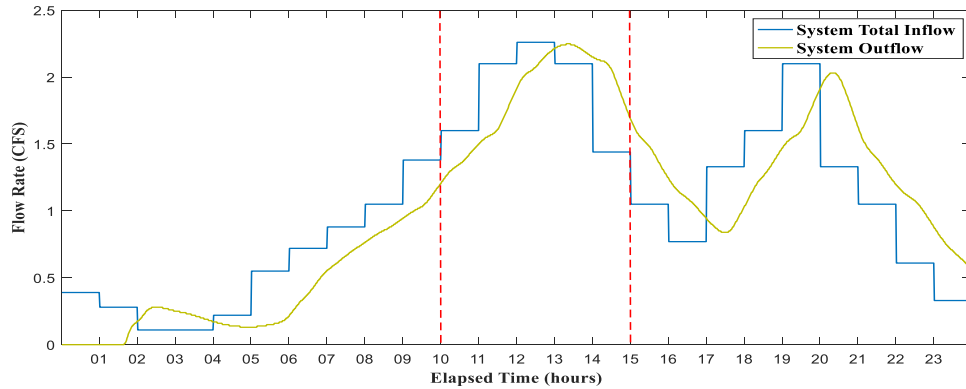
403

404 Figure 8: Comparison of GRA results obtained from proposed selection method and all possible scenarios
 405 simulation for the real sewer network.

406 **3.3 Evaluation of the Toolbox**

407 In the final evaluation, out of 1005 existing conduits, 275 conduits (network skeleton) were
 408 selected to be participated in analyzing global resilience by the toolbox. These conduits consisted
 409 of main transmission line, collectors and pipes in the main streets which selected based on an
 410 engineering judgment. Noteworthy that all conduits were participated in the network simulation
 411 but the link blockage (failure) was assumed to be occurred in these 275 conduits.

412 A standard sewage daily pattern was used to determine the peak time of sewage inflow to
 413 evaluate the network performance in critical situations. Figure 9 shows the dry weather inflow and
 414 the outfall diagrams in which the highest rate of network input occurs in the time interval from 10
 415 am to 3 pm. Therefore, at this time interval in each scenario simulation, the roughness of selected
 416 conduits was increased to 100 during runtime by using “swmm_setConduitLinkRoughness”
 417 exportable function of O-SWMM API.



418

419

Figure 9: Dry weather inflow and the outfall diagrams. The dashed red lines show failure interval

420

In this experiment, simulating the total number of all possible scenarios could take long time,

421

because all 275 conduits were participated in analyzing global resilience. Therefore, performance

422

of proposed scenarios selection method was evaluated by comparing it's results with GRA results

423

obtained using random scenarios selection method proposed by Mugume et al. (2015). To analyze

424

the global resilience, Mugume et al. (2015) used a convergence analysis to determine the minimum

425

required number of scenarios for different failure levels. For a comprehensive comparison, this

426

convergence method was also performed in this section to determine the value of S , in our

427

proposed method.

428

3.3.1 Convergence Analysis

429

For convergence analysis and determining the value of S , the following steps were taken.

430

1) Seven different set were simulated which are: 5 random sequences (5 scenarios \times 275

431

failure levels), 10 (2750 failure scenarios), 25 (6,875 failure scenarios), 50 (13,750 failure

432

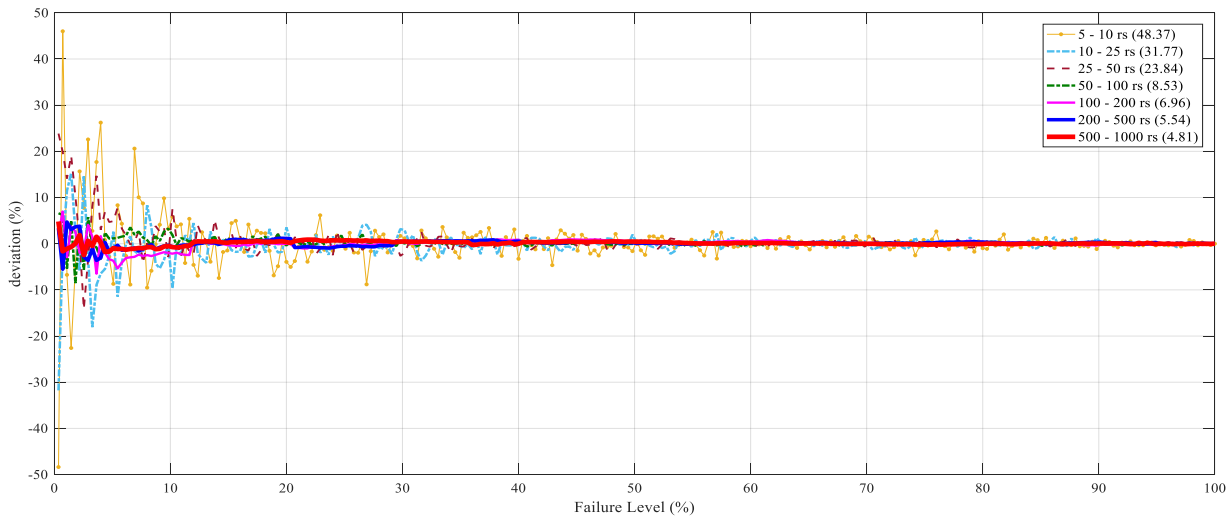
scenarios), 100 (27500 failure scenarios), 200 (55,000 failure scenarios), 500 (137,500

433

failure scenarios), 1000 (275000 failure scenarios).

- 434 2) The mean of the total flood volume in each failure level was determined for all random
 435 sequence sets.
- 436 3) The percentage deviation between each consecutive set was calculated based on the
 437 computed mean values, i.e., deviation between {5,10}; {10, 25}; {25,50}; {50,100};
 438 {100,200}; {200,500}; {500,1000}.

439 Figure 10 shows the result of convergence analysis for the sets. For the first time, a convergence
 440 was obtained in set {50,100}. The maximum deviation of this set was 8.53%. In the three other
 441 sets, the maximum deviation was also reduced to 6.96%, 5.54% and 4.81%, respectively.



442

443 Figure 10: Convergence of GRA results for random links failure sequences

444 3.3.2 Performance Evaluation

445 Based on the obtained deviation results, the value of S was considered as 1000. The value of
 446 k_{TF} like previous experiments was set to 0.1; thus 200 strategical scenarios (100-minimum and
 447 100-maximum points of RW fitness function) participated in selecting scenarios of the next failure
 448 level to generate first set of scenarios. Moreover, 1000 scenarios in each failure level were selected
 449 randomly in order to generate second set of scenarios. To evaluate the performance of the proposed

450 scenario selection method, the GRA results of two generated sets are shown in fig. 11, separately.

451 The results showed that the minimum and maximum of GRA calculated by the proposed method

452 are significantly different from random selection results. The pattern of mean resilience resulted

453 by using these two methods is also different. In the random selection results, the mean resilience

454 has an increasing trend from 28% to 53% of failed links. But, the mean resilience in the proposed

455 selection method has a sharp decrease at around 60% of failed links and before and after this point

456 the resilience is decreasing with a slight slope. A convergence analysis method was used to

457 determine the minimum required number of scenarios for each failure level, but finding and

458 considering the extremum points of the resilience in each failure level can make more accurate

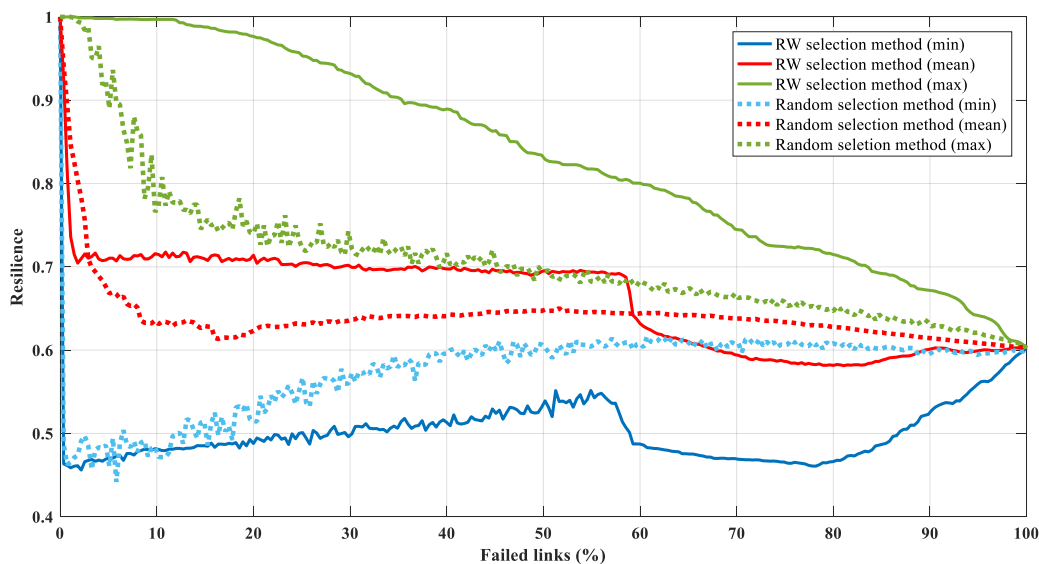
459 GRA result, when a trade-off between execution time and reliability of result is inevitable.

460 Moreover, the equation 2 is only used to calculate resilience of scenarios selected by two methods

461 in order to compare their GRA results. But if another model (formula) is used to calculate the

462 resilience, the variables of that formula should be used as criteria in TOPSIS, when our proposed

463 scenario selection method is used.



464

465 Figure 11: Comparison of GRA results generated using the proposed roulette wheel and the random selection
 466 methods

467 Simulation of each failure scenario of the real sewer network alone takes 107 seconds, if the
468 original SWMM is used. According to 275 conduits, the total number of all possible scenarios is
469 around $6.07 e + 82$ and simulating this number of scenarios could take long time around $9 e + 75$
470 years. But, $2.75e5$ failure scenarios were only simulated by presented GRA toolbox based on RW
471 scenario selection method. If the original SWMM is used, simulating this number of scenarios in
472 parallel manner takes about 34 days, using 10 logical processors. But the proposed toolbox
473 analyzed global resilience of the network just in 15 days using O-SWMM API which reduced the
474 execution time by 56% (2.26 times faster).

475 **4. Conclusions**

476 In this article, an open-source toolbox was presented for investigating functional resilience in
477 sewer networks based on GRA. To properly cover the large space of failure scenarios that is a
478 challenge in the real networks, a simple method is proposed based on the roulette wheel to identify
479 the most strategical combination of failed pipes in each failure level. For two case studies (sample
480 and real networks), the global resilience was estimated by simulating a small number of scenarios
481 with RMSE 0.025 and 0.022 comparing with simulating all possible scenarios. Moreover, using
482 O-SWMM API which is an optimized development of EPA's SWMM, the GRA execution was
483 2.5 and 2.26 times faster.

484 The proposed API provides the ability to modify roughness and links properties during
485 simulation to simulate quantitative failures. Future work will focus on developing O-SWMM API
486 to modify quality parameters in order to analyze global resilience of the system to sewage quality
487 disturbance.

488

489 **References**

- 490 Almoghatawi, Y., Barker, K., & Albert, L. A. (2019). Resilience-driven restoration model for interdependent
491 infrastructure networks. *Reliability Engineering & System Safety*, 185, 12-23.
492 <https://doi.org/10.1016/j.ress.2018.12.006>.
- 493 Atashi, M., Ziaei, A. N., Khodashenas, S. R., & Farmani, R. (2020). Impact of isolation valves location on
494 resilience of water distribution systems. *Urban Water Journal*, 1-8. <https://doi.org/10.1080/1573062X.2020.1800761>.
- 495 Banik, B. K., Di Cristo, C., & Leopardi, A. (2014). SWMM5 Toolkit Development for Pollution Source
496 Identification in Sewer Systems. *Procedia Engineering*, 89, 750-757. <https://doi.org/10.1016/j.proeng.2014.11.503>.
- 497 Burger, G., Sitzenfrei, R., Kleidorfer, M., & Rauch, W. (2014). Parallel flow routing in SWMM 5. *Environmental
498 Modelling & Software*, 53, 27-34. <https://doi.org/10.1016/j.envsoft.2013.11.002>.
- 499 Burgess, E., Magro, W. R., Clement, M., Moore, C., & Smullen, J. J. (2000). Parallel Processing Enhancement to
500 SWMM/EXTRAN. *Journal of Water Management Modeling*, 206(03), 45-60. <http://doi:10.14796/JWMM.R206-03>.
- 501 Butler, D., Farmani, R., Fu, G., Ward, S., Diao, K., Astaraie-Imani, M. (2014). A new approach to urban water
502 management: Safe and sure. *Procedia Engineering*, 89, 347–354. <https://doi:10.1016/j.proeng.2014.11.198>.
- 503 Butler, D., Ward, S., Sweetapple, C., Astaraie Imani, M., Diao, K., Farmani, R., & Fu, G. (2016). Reliable, resilient
504 and sustainable water management: The Safe & SuRe approach. *Global Challenges*, 1(1), 63-77.
505 <https://doi.org/10.1002/gch2.1010>.
- 506 Cai, B., Zhang, Y., Wang, H., Liu, Y., Ji, R., Gao, C., Kong, X. & Liu, J. (2021). Resilience evaluation
507 methodology of engineering systems with dynamic-Bayesian-network-based degradation and maintenance.
508 *Reliability Engineering & System Safety*, 209, 107464. <https://doi.org/10.1016/j.ress.2021.107464>.
- 509 Chen, C., Yang, M., & Reniers, G. (2021). A dynamic stochastic methodology for quantifying HAZMAT storage
510 resilience. *Reliability Engineering & System Safety*, 215, 107909. <https://doi.org/10.1016/j.ress.2021.107909>.
- 511 Cheng, Y., Elsayed, E. A., & Huang, Z. (2021). Systems resilience assessments: a review, framework and metrics.
512 *International Journal of Production Research*, 1-28. <https://doi.org/10.1080/00207543.2021.1971789>.
- 513 Davis, P., Sullivan, E., Marlow, D., & Marney, D. (2013). A selection framework for infrastructure condition
514 monitoring technologies in water and wastewater networks. *Expert Systems with Applications*, 40(6), 1947-1958.
515 <https://doi.org/10.1016/j.eswa.2012.10.004>.
- 516 Diao, K., Sweetapple, C., Farmani, R., Fu, G., Ward, S., & Butler, D. (2016). Global resilience analysis of water
517 distribution systems. *Water research*, 106, 383-393. <https://doi.org/10.1016/j.watres.2016.10.011>.

518 Doorn, N., Gardoni, P., & Murphy, C. (2019). A multidisciplinary definition and evaluation of resilience: The role
519 of social justice in defining resilience. *Sustainable and Resilient Infrastructure*, 4(3), 112-123.
520 <https://doi.org/10.1080/23789689.2018.1428162>.

521 Gironás, J., Roesner, L. A., Rossman, L. A., & Davis, J. (2010). A new applications manual for the Storm Water
522 Management Model (SWMM). *Environmental Modelling & Software*, 25(6), 813-814.
523 <https://doi.org/10.1016/j.envsoft.2009.11.009>.

524 Hosseini, S., K. Barker, and J.E. Ramirez-Marquez. (2016). A review of definitions and measures of system
525 resilience. *Reliability Engineering and System Safety*, 145: 47-61. <http://dx.doi.org/10.1016/j.res.2015.08.006>.

526 Hughes, J., Cowper-Heays, K., Olesson, E., Bell, R., & Stroombergen, A. (2020). Impacts and implications of
527 climate change on wastewater systems: A New Zealand perspective. *Climate Risk Management*, 100262.
528 <https://doi.org/10.1016/j.crm.2020.100262>.

529 Hwang, C. L., Lai, Y. J., & Liu, T. Y. (1993). A new approach for multiple objective decision making. *Computers
530 & Operations Research*, 20(8), 889-899.

531 Johnson, C. A., Flage, R., & Guikema, S. D. (2021). Feasibility study of PRA for critical infrastructure risk
532 analysis. *Reliability Engineering & System Safety*, 212, 107643. <https://doi.org/10.1016/j.res.2021.107643>.

533 Johansson, J., Hassel, H., & Cedergren, A. (2011). Vulnerability analysis of interdependent critical infrastructures:
534 case study of the Swedish railway system. *International Journal of Critical Infrastructures*, 7(4), 289-316.
535 <https://doi.org/10.1504/IJCIS.2011.045065>.

536 Long, Y., Yang, Y., Lei, X., Tian, Y., & Li, Y. (2019). Integrated assessment method of emergency plan for sudden
537 water pollution accidents based on improved TOPSIS, Shannon entropy and a coordinated development degree model.
538 *Sustainability*, 11(2), 510. <https://doi.org/10.3390/su11020510>.

539 Macro, K., Matott, L. S., Rabideau, A., Ghodsi, S. H., & Zhu, Z. (2019). OSTRICH-SWMM: A new multi-
540 objective optimization tool for green infrastructure planning with SWMM. *Environmental Modelling & Software*,
541 113, 42-47. <https://doi.org/10.1016/j.envsoft.2018.12.004>.

542 Maghsoodi, A. I., Abouhamzeh, G., Khalilzadeh, M., & Zavadskas, E. K. (2018). Ranking and selecting the best
543 performance appraisal method using the MULTIMOORA approach integrated Shannon's entropy. *Frontiers of
544 Business Research in China*, 12(1), 2.

545 Mair, M., Sitzenfrei, R., Kleidorfer, M., & Rauch, W. (2014). Performance improvement with parallel numerical
546 model simulations in the field of urban water management. *Journal of Hydroinformatics*, 16(2), 477-486.
547 <https://doi.org/10.2166/hydro.2013.287>.

548 Martínez-Solano, F. J., Iglesias-Rey, P. L., Saldarriaga, J. G., & Vallejo, D. (2016). Creation of an SWMM toolkit
549 for its application in urban drainage networks optimization. *Water*, 8(6), 259. <http://doi.org/10.3390/w8060259>.

550 Mottahedi, A., Sereshki, F., Ataei, M., Qarahasanlou, A. N., & Barabadi, A. (2021). Resilience estimation of
551 critical infrastructure systems: application of expert judgment. *Reliability Engineering & System Safety*, 107849.
552 <https://doi.org/10.1016/j.ress.2021.107849>.

553 Mugume, S. N., & Butler, D. (2016). Evaluation of functional resilience in urban drainage and flood management
554 systems using a global analysis approach. *Urban Water Journal*, 14(7), 727-736.
555 <https://doi.org/10.1080/1573062X.2016.1253754>.

556 Mugume, S.N., Gomez, D.E., Fu, G., Farmani, R., Butler, D., (2015). A global analysis approach for investigating
557 structural resilience in urban drainage systems. *Water Research*. 81, 15–26.
558 <https://doi.org/10.1016/j.watres.2015.05.030>.

559 Nan, C., & Sansavini, G. (2017). A quantitative method for assessing resilience of interdependent infrastructures.
560 *Reliability Engineering & System Safety*, 157, 35-53. <http://dx.doi.org/10.1016/j.ress.2016.08.013>.

561 Riaño-Briceño, G., Barreiro-Gomez, J., Ramirez-Jaime, A., Quijano, N., & Ocampo-Martinez, C. (2016).
562 MatSWMM—An open-source toolbox for designing real-time control of urban drainage systems. *Environmental*
563 *Modelling & Software*, 83, 143-154. <https://doi.org/10.1016/j.envsoft.2016.05.009>.

564 Shannon, C. E. (1948). A mathematical theory of communication. *The Bell System Technical journal*, 27(3), 379-
565 423.

566 Sharma, N., Tabandeh, A., & Gardoni, P. (2018). Resilience analysis: A mathematical formulation to model
567 resilience of engineering systems. *Sustainable and Resilient Infrastructure*, 3(2), 49–67.
568 <http://dx.doi.org/10.1080/23789689.2017.1345257>.

569 Sweetapple, C., Diao, K., Farmani, R., Fu, G., & Butler, D. (2018, July). A tool for global resilience analysis of
570 water distribution systems. WDSA/CCWI Joint Conference 2018. <http://hdl.handle.net/2086/16499>.

571 Sweetapple, C., Astaraie-Imani, M., & Butler, D. (2018). Design and operation of urban wastewater systems
572 considering reliability, risk and resilience. *Water research*, 147, 1-12. <https://doi.org/10.1016/j.watres.2018.09.032>.

573 Wang, M., Sweetapple, C., Fu, G., Farmani, R., & Butler, D. (2017). A framework to support decision making in
574 the selection of sustainable drainage system design alternatives. *Journal of Environmental Management*, 201, 145-
575 152. <https://doi.org/10.1016/j.jenvman.2017.06.034>.

576 Wang, S., Fu, J., & Wang, H. (2019). Unified and rapid assessment of climate resilience of urban drainage system
577 by means of resilience profile graphs for synthetic and real (persistent) rains. *Water research*, 162, 11-21.
578 <https://doi.org/10.1016/j.watres.2019.06.050>

579